Final Draft
of the original manuscript

Tamoffo, A.; Vondou, D.; Pokam, W.; Haensler, A.; Yepdo, Z.; Fotso-Nguemo, T.; Djiotang Tchotchou, L.; Nouayou, R.:

Daily characteristics of Central African rainfall in the REMO model.

In: Theoretical and Applied Climatology. Vol. 137 (2019), 2351 - 2368.

First published online by Springer: 02.01.2019

https://dx.doi.org/10.1007/s00704-018-2745-5

Daily characteristics of Central African rainfall in the REMO model

Alain T. Tamoffo · Derbetini A. Vondou · Wilfried M. Pokam · Andreas Haensler · Zéphirin D. Yepdo · Thierry C. Fotso-Nguemo · Lucie A. Djiotang Tchotchou · Robert Nouayou

Abstract In this paper, daily characteristics of the Central Africa rainfall are assessed using the regional model REMO in the framework of contributions to the CORDEX-Africa project. The model is used to dynamically downscale two global climate models (MPI-ESM-LR and EC-EARTH) for the present (1981–2005) and future (2041–2065, 2071–2095) climate under the Representative Concentration Pathways (RCPs) 2.6, 4.5 and 8.5 emission scenarios. A substantial spatio-temporal variability of the daily precipitation characteristics is obtained, as well as varying inferences for individual indices. For the present days, both REMO's runs capture reasonably well the mean seasonal rainfall, the frequency of wet days, the threshold of extreme rainfall and the cumulative frequency of daily rainfall. The model better simulates the frequency of rainy days than their intensity. It is found that origins of model biases

Alain T. Tamoffo, Derbetini A. Vondou, Wilfried M. Pokam, Zéphirin D. Yepdo, Thierry C. Fotso-Nguemo, Lucie A. Djiotang Tchotchou
Laboratory for Environmental Modelling and Atmospheric Physics (LEMAP), Department of Physics, University of Yaounde 1, P.O. Box 812 Yaounde, Cameroon
E-mail: alaintamoffotchio@gmail.com

Alain T. Tamoffo, Derbetini A. Vondou, Wilfried M. Pokam
2LMI DYCOFAC (IRD, University of Yaoundé, IRGM), IRD BP1857, Yaoundé Cameroun

Wilfried M. Pokam
Department of Physics, Higher Teacher Training College, University of Yaounde 1, P.O. Box 47 Yaounde, Cameroon

Andreas Haensler
Climate Service Center Germany (GERICS), Helmoltz-Zentrum Geesthacht, Fischertwiete 1, Hamburg, Germany

Zéphirin D. Yepdo, Thierry C. Fotso-Nguemo
Climate Change Research Laboratory, National Institute of Cartography, P.O. Box 157, Yaounde, Cameroon

Robert Nouayou
Laboratory of Geophysics and Geoexploration, Department of Physics, University of Yaounde 1, P.O. Box 812 Yaounde, Cameroon

differ as a function of regions. Over the continent, boundary conditions tend to influence the spatial distribution of rainfall whereas over oceanic and coastal regions, REMO's physics seems to dominate over the boundary forcing. The projected frequency of wet days shows a decrease along the 21st century over most part of the continent. Throughout the century, all scenarios of REMO decrease the rate of rainfall with increasing intensity, and which will be noticeable in the Sahelian region at late 21st century. Furthermore, the extreme events threshold decrease over sahelian regions and increase along the coastal regions.

Keywords Frequency of wet days · Frequency distribution · Threshold of extreme events · RCPs · Central Africa · REMO

1 Introduction

Industrial emission and continual growth of the world's population increase anthropogenic contribution to climate change and climate variability (IPCC, 2007). Developing regions such as Central Africa (CA) are the most vulnerable to these changes due to their dependence on agriculture, forestry and water resources. These vital sectors of their economy are strongly affected by extreme climate events such as floods and droughts. For example, the shrinking of the area of Lake Chad in the order of 90% (Gao et al, 2011), due to extreme drought and increased irrigation withdrawals (Birkett, 2000). Recent studies have demonstrated that population expansion and climate change have significantly contributed to the decline of the Central African forest and vegetation greenness (Malhi, 2018; Garcin et al, 2018). Furthermore, Hua et al (2018) have shown a critical long-term drought over the Congo basin by exploring multiple reanalysis datasets and climate modeling experiments. Consequently, a simulated decrease in precipitation will lead to a reduction in runoff in the Congo Basin in line with previous findings of Aloysius and Saiers (2017). On the basis of a multitude of global and regional climate models, a study of Haensler et al (2013) suggest a consistently increasing temperature over CA across the 21st century. Further, the rate of warming has a strong seasonal response as they reported.

Investigations found out that global circulation models (GCMs) have difficulties in capturing the regional features of CA climate. GCMs from the Coupled Model Intercomparison Project Phase 5 (CMIP5, Taylor et al, 2012) show a low consensus of simulated rainfall (Haensler et al, 2013; Creese and Washington, 2016, 2018). Aloysius et al (2015) have highlighted that most CMIP5 models are less successful in simulating seasonal cycle, spatial pattern and intensity of rainfall due to the weak Atlantic teleconnection and SST fluctuation. Significant heterogeneities have been reported in GCMs rainfall, some models show rainfall maxima in the west, other in the east part (Washington et al, 2013; Creese and Washington, 2018). They project increases in precipitation in the eastern sector, whereas they project decreases in the western sector (James et al, 2013), added to their poor performance to reproduce heavy rainfall events (Fotso-Nguemo et al, 2018). The horizontal grid spacing is generally cited as one probable reason for such behaviour (Dosio et al, 2015). They are too coarse to explicitly represent the regional counterpart of atmospheric weather systems. Regional climate models (RCMs) may offer much more rational characterizations of the climate state and variability over a wide range of spatio-temporal scales. Using RCM to appreciate behavior of change in precipitation make necessary that the model reasonably simulate the statistics of daily precipitation as well as the physical mechanisms that produce these precipitation. The recent downscaling of multiple GCMs from CMIP5 gives possibility to further investigate the central African climate through the second phase of the African branch of the COordinated Regional climate Downscaled EXperiment project (CORDEX-Africa, Giorgi et al, 2009) Project. CORDEX-Africa datasets are perhaps the most reliable tool to scrutinize CA climate where in-situ observations are very sparse. Although consistent dissimilarities between results from RCMs and observations may not necessarily be less than those for GCMs (Dosio et al, 2015), many studies conducted in the framework of CORDEX-Africa have shown added value of RCMs over CA (Dosio et al, 2015; Fotso-Nguemo et al, 2017; Vondou and Haensler, 2017).

Pokam et al (2018) found that regional warming greatly differs between 1.5°C and 2°C global warming levels with a significant increase in consecutive dry days. In relation to the different levels of global warming, the exploration of the sequence of dry/wet days in a year using a robust assessment of multiple CORDEX models also resulted in a drying trend over much part of CA. Vondou and Haensler (2017) showed that increasing REMO horizontal resolution could affect precipitation statistics and improve representation of the circulation. In the studies referenced above, the evaluation of RCMs was done with a special focus on mean temperature and precipitation climatology. Since climate models are used to predict future changes in extreme precipitation in response to global warming, it is important to know how well they simulate observed changes in daily indices that are associated with warming over CA. Thus further researches are needed to better address the topic.

Daily rainfall features of precipitation are relevant in many sectors such as the dynamic of the soil moisture, hydrology, evaporation and flow. Unfortunately, investigations exploring in detail into daily rainfall characteristics in RCM outputs are missing over CA. Only few authors have been interested in the study of these properties of precipitation (Fotso-Nguemo et al, 2016, 2017; Vondou and Haensler, 2017; Pokam et al, 2018). Assessing these behaviors of daily rainfall statistics is important in RCM evaluation researches. The present study investigates precipitation over CA as simulated by REMO driven by two GCMs. The goal is to evaluate the performances of the regional climate model REMO in simulating daily rainfall characteristics over CA through some climate parameters mentioned above, and then present their climate change projections at the mid (2041-2065) and late (2071-2095) 21^{st} century, under three representative concentration pathway scenarios (RCPs, Moss et al. 2010): RCP2.6, RCP4.5 and RCP8.5. The paper is organized as follows: The model configuration, data used and methodology are described in Section 2. Section 3 presents the results and discussion. Concluding statements are provided in Section 4.

2 Model description and methods

2.1 Model description and simulation process

REMO uses a revised version of the physics parameterization of GCM ECHAM4 (Lohmann and Roeckner, 1996). It has been implemented in the CORDEX-Africa domain to resolve atmospheric phenomena not included in GCMs and it is based on the Europa-Model system of the German Climate Service (Majewski, 1991). The equations of finite-difference are solved on an Arakawa C-grid (Jacob and Podzun, 1997). Some specifications of REMO model are summarized in Table 1 and more information are available in Saeed et al (2013); Teichmann et al (2013); Weber et al (2017).

Historical simulations of REMO model were conducted from 1950 to 2005, considering as constant the value of natural and anthropogenic forcing (Saeed et al, 2013). Climate projections were performed using RCPs (2.6, 4.5 and 8.5) scenarios from 2006 to 2100. In this work, the RCM REMO is used to singly dynamically downscale two GCMs (from `r1i1p1` member) at $\sim 50km$ horizontal resolution: the Europe wide Consortium Earth System Model (EC-Earth; `http://ecearth.knmi.nl`) and the lower resolution of the Max Planck Institute-Earth System Model (MPI-ESM; `http://www.mpimet.mpg.de/en/science.html`). Subsequently, we use the terms REMO-EC and REMO-MPI to designate respectively forcings using EC-Earth and MPI-ESM GCMs as boundary conditions. For each output, three 25-yr time frames were used: $1981-2005$ for historical; $2041-2065$ and $2071-2095$ for projections.

2.2 Observational datasets

Assessment of REMO's skills is based on the comparison between REMO's experiments and multiple observational datasets so as to account for uncertainties in observed products (Nikulin et al, 2012; Diallo et al, 2012; Sylla et al, 2013). Brief details of all observed data used in this study are as follows:

• The Global Precipitation Climatology Project dataset (GPCP-1DD, 1997 to 2005, daily time scale, $1^\circ \times 1^\circ$ resolution, Huffman et al. 1997). GPCP rainfall results of the combination of several rain-gauge stations, satellite geostationary and low-orbit infrared estimations.

• The Climate Hazards Group InfraRed Precipitation with Stations (CHIRPS, 1981 to 2005, daily product, $0.05^\circ \times 0.05^\circ$ grid space, Funk et al. 2014). Produced by U.S. Geological Survey (USGS) and University of California, Santa Barbara (UCSB) scientists, CHIRPS combines new resources of satellite observations, mean precipitation from stations, and rainfall predictors such as altitude, latitude and longitude.

• The Tropical Rainfall Measuring Mission 3B42 (TRMM, 1998 to 2005, tri-3B42 hourly, $0.25^\circ \times 0.25^\circ$ horizontal resolution, Huffman and Bolvin. 2013). TRMM rainfall is generated by a combination of microwave-infrared estimations and monthly combined microwave-infrared-gauge estimates of global precipitation.

The study area is presented in Fig 1. For regional analyses, five homogeneous climatic regions (Reg 1, Reg 2, Reg 3, Reg 4 and Reg 5; see blue boxes in Fig. 1), previously used in Fotso-Nguemo et al (2016) have been selected, based on Köeppen Geiger's climate classification.

2.3 Methods

The REMO model evaluation is done on a 25-yr period (1981 to 2005). Mean rainfall climatology, seasonal frequency and intensity of wet days, frequency distribution and cumulative frequency of daily rainfall intensity as well as threshold of extreme events are analysed. In order to perform the comparison between several datasets, all data are re-mapped onto GPCP grid. Mean Bias (MB), Pattern Correlation Coefficient (PCC) and Root Mean Square Difference (RMSD) have been computed to assess systematic errors and skills of the model. They were computed as follows:

$$MB = \frac{1}{N}\sum_{i=1}^{N}(x_i - y_i) \tag{1}$$

$$PCC = \frac{1}{\sigma_x \sigma_y}\left[\frac{1}{N}\sum_{i=1}^{N}(x_i - \overline{x})(y_i - \overline{y})\right] \tag{2}$$

$$RMSD = \left[\frac{1}{N}\sum_{i=1}^{N}(x_i - y_i)^2\right]^{1/2} \tag{3}$$

where N is the number of grid points, x_i and y_i are respectively the values of the variable to the i^{th} grid point of the model and observation. $\overline{x}$ and $\overline{y}$ are respectively their mean values, σ_x and σ_y are their standard deviations defined as follows:

$$\sigma_x = \sqrt{\frac{1}{N}\sum_{i=1}^{N}(x_i - \overline{x})^2} \qquad and \qquad \sigma_y = \sqrt{\frac{1}{N}\sum_{i=1}^{N}(y_i - \overline{y})^2} \tag{4}$$

Some hydro-climatic indices to characterize daily precipitation in Central African region are analysed. These include:

- The seasonal frequency of wet days is obtained by the ratio of total days of season where rainfall amount ≥ 1 mm ($RR \geq 1$ mm) by the total number of days of the considered season.
- The simple daily index intensity (SDII) is obtained by considering the mean intensity of daily rainfall events as follows.

$$SDII_i = \frac{\sum_{n=1}^{N} RR_{ni}}{N} \tag{5}$$

where N is the number of wet days in i period and n is the daily rainfall amount (RR $\geq$ 1 mm).

- The frequency distribution and cumulative frequency of the simulated rainfall intensity of a range is the ratio of the accumulated precipitation of considered range by the total precipitation.
- The threshold of extreme events is defined at a grid point as the 90^{th} percentile of the total annual precipitation fallen at this point. Therefore, we evaluate the capacity of the models to simulate these extremes and thresholds.

The climate change signal is defined through the difference in mean values of the future to the baseline period considering the various RCPs warming scenarios. Thereby, for a given variable X (rainfall, wet days), the climate change signal is obtained as follows:

$$CC(X) = \frac{X_{future} - X_{present}}{X_{present}} \times 100 \tag{6}$$

3 Results and discussion

3.1 Current climate assessment

It is helpful to study the ability of a model to reproduce current climatology in order to help increase the reliability of projected changes. Therefore, this section focuses on the results of REMO model simulations under baseline period.

3.1.1 Mean-seasonal rainfall climatology

Over CA, rainfall generation is strongly influenced by the north-south excursion of the Inter-Tropical Convergence Zone (ITCZ), which controls the alternation of wet and dry seasons (Jackson et al, 2009; Nicholson and Grist, 2003). For a better characterization of simulated daily rainfall in the central African region, RCMs must well depict the seasonal positions and strength of ITCZ. Figure 2 shows the daily mean rainfall over CA for December-February (DJF), March-May (MAM), June-August (JJA) and September-November (SON) seasons. Model biases are shown in Fig. 3.

Generally, both outputs capture seasonal evolutions of ITCZ although some dry and wet biases are still present over the domain (Fig 2). Magnitudes GPCP and CHIRPS show a high level of agreement with few biases ($\pm$1 mm/day). However for all seasons, larger differences appear between observations and RCM runs, too pronounced over the Ocean and coastal regions where the two REMO's experiments more extend the ITCZ area with significant wet biases $\sim$8 mm/day. This behavior has been linked by Hernández-Díaz et al (2013) to inadequacies in the parameterization of boundary layer and subgrid-scale vertical transport processes. The fact that the two experiments present a similar response to the different forcings suggests that the role of the REMO's internal physics is dominant (Diallo et al, 2016). Over the continental part, biases are relatively low. Slight wet biases are found over forested southern Cameroon, Congo, Gabon, Democratic Republic of Congo (DRC) and dry biases over the remaining domain. Recently, a similar result was found by Dosio et al (2015) over CORDEX-Africa domain using another RCM. They assigned this failure of CCLM to their structural biases which may be related to soil parameterization. Coppola et al (2014) have also argued that RCMs discrepancies could likewise be derived from differences in large scale circulation patterns, the natural variability and the simulation of surface water and energy budgets. Some differences among experiment estimates can be noticed as function of the location, spatial extent, and magnitude of the precipitation maxima. For example in the east of the study area, REMO-EC is close to observations whereas REMO-MPI overestimates the magnitude of simulated precipitation. This suggests that the Lateral boundary condition (LBC) errors contribute to the biases exhibited by REMO. In this case, differences between the two simulations can be explained by the errors transmitted originally by the different internal dynamics and physical schemes of GCMs (Endris et al, 2016). For instance, the land surface scheme of EC-Earth is HTESSEL, based on the model cycle 31r1 (Van Noije et al, 2014). Its convective scheme was updated to the formulations of cycle 32r3 and produced the higher convective activity over land, then improving the tropical rainfall (Bechtold et al, 2008). On the other hand, MPI-ESM is coupled to ocean model MPI-OM (Mikolajewicz et al, 2010), to dynamic process models for marine biogeochemistry, the Hamburg Model of Ocean Carbon Cycling HAMOCC5 (Ilyina et al, 2013) and the Jena Scheme for Biosphere-Atmosphere Coupling in Hamburg JSBACH (Reick et al, 2013). Generally, REMO have difficulties to simulate land-sea surface transition. This behavior has also been reported by Fotso-Nguemo et al (2016), who have found that the model's performances degrade compared to CMAP rainfall.

Statistical parameters of seasonal rainfall are summarized in Table 2. Experiment scores are better when compared to CHIRPS and GPCP (with values of PCC/RMSD $\sim$0.94/2.01 for REMO-EC and 0.93/1.68 for REMO-MPI) than TRMM (0.70/2.73 for REMO-EC and 0.70/2.74 for REMO-MPI). Similar results were also found by Dosio et al (2015) over CORDEX-Africa using CCLM. This imply the existence of discrepancies in observed products (Nikulin et al, 2012; Sylla et al, 2013; Panitz et al, 2014). Moreover, Sylla et al (2013) and Giorgi et al (2014) have linked this deficiency to the fact that TRMM produces much intense rainfall events than GPCP.

3.1.2 Intensity and frequency of wet days

In this section, the focus is on daily rainfall events by analysing frequency of wet days (Fig. 4) and simple daily intensity index (Fig 5). It is found that CHIRPS produces higher frequency of wet days than GPCP and TRMM (see rows 1-3 in Fig 4). The reverse situation prevails for the intensity of daily rainfall events. Patterns of the coarse-resolution GPCP are close to high-resolution TRMM. Maximums of seasonal intensity and frequency generally correspond to that of mean rainfall found in Fig 2. This result was also reported by Sylla et al (2015) over West Africa.

Simulations well depict the frequency of rainy days with high PCC ≥ 0.70 and low MB $< 16\%$ for all seasons with respect to all observations (see Table 3). The two runs fairly reproduce the spatial distribution of intensity of daily rainfall events with some differences over oceanic regions (Fig 5). They show strong wet biases with respect to CHIRPS and generally low PCC (see Table 4) whereas MB are relatively lower compared to other observations. However, as shown in Figure 5, strong wet biases are located over oceanic and coastal regions.

Overall, biases of mean frequency and intensity of rainfall show a similar trend. This highlight that the structure of intensity of mean precipitation over CA is due to frequency and intensity of daily precipitation events, but the contribution of intensity is higher. While observations differ with regard to intensity and frequency of rainfall events, RCM runs provide consistent information for the two indices, thus confirming the influence of the regional signal over the LBC.

3.1.3 Threshold of extreme rainfall

Figure 6 represents the extreme precipitation threshold characterized by the 90^{th} percentile of total rainfall. It shows a high rate of agreement among observations with high PCC $\geq$ 0.94 with respect to CHIRPS. However, some discrepancies still exist. Largest threshold values are found along coastal regions and vicinity of mount Cameroon $\sim$31 mm/day in TRMM, $\sim$24 mm/day in GPCP and $\sim$22 mm/day in CHIRPS and lowest in the sahelian region $\sim$2 mm/day. Over coastal regions, largest values of threshold can be linked to the high convective activity over the guinea golf and topographic effects. Abiodun et al (2015) have also found that TRMM produces higher extreme rainfall threshold than GPCP. They have assigned this discrepancy to the difference in the spatial resolution between the two datasets. The strong threshold values have likewise been found over DRC and can be associated to the greater number of rainfall events (Jackson et al, 2009; Vondou and Haensler, 2017).

RCM runs are remarkably close to observations with good PCC $\geq$ 0.78 and where REMO-EC slightly outperforms than REMO-MPI. They capture well the strong threshold values located along the coastal inland regions with a slight overestimation and eastward extension, more pronounced in REMO-EC. However, there are robust disagreements above the oceanic part where both runs strongly overate the threshold of extreme events with maxima $\sim$53 mm/day in REMO-MPI and $\sim$50 mm/day in REMO-EC. As earlier found, the two forcings produce a larger number and intensity of daily rainfall events on the oceanic part, which may explain the high threshold of extreme events. Recently with a multitude of RCMs, Klutse et al (2016) also found that UQAM-CRCM, DMI-HIRHAM, UC-WRF and MPI-REMO overestimate high values of heavy rainfall over oceanic regions.

3.1.4 Cumulative frequency of daily rainfall

To get an insight of how RCM runs split the daily rainfall, distributed and cumulative frequency in CA and in homogeneous regions are used (Fig 7). The horizontal line indicates the 90^{th} percentile of total rainfall and whose intersections with curves show the threshold of heavy rainfall events. All datasets provide congruent information in decreasing rainfall frequency with an increasing intensity. Except for Reg 1, they are close for intensities less than 10 mm/day. Disparities appear for high intensities of rainfall, then gradually vanish. Greatest discrepancies occur with rainfall intensity within the range 20-40 mm/day. For the whole CA and all homogeneous regions excluding Reg 1, GPCP and CHIRPS are closer and generally show the fastest decrease rates relative to TRMM while this later is rather close to simulations. In Reg 1, experiments are close to CHIRPS for low rainfall intensities (Fig 7b). In regard of higher intensities, they are rather close to GPCP and TRMM. For the 90^{th} percentile threshold ($R90$), TRMM is similar to those simulated. For the whole CA and Reg 4 illustrated in Fig 7a and e, both runs overestimate $R90$ ($R90 \sim 47$ mm/day). A similar situation occurs in Reg 5 (Fig 7f) but with relative weak $R90$ ($R90 \sim 33$ mm/day). In other sub-regions, RCM runs underestimate $R90$ compared to TRMM. Overestimation is obtained with respect to GPCP and CHIRPS ($R90 \sim 30$ mm/day in Reg 1 and Reg 3; $R90 \sim 37$ mm/day in Reg 2).

3.2 Climate change projections

3.2.1 Change in frequency of wet days

Projected changes in the spatial pattern of wet days (in %) for the mid (2041–2064 minus 1981–2005) and late (2071–2095 minus 1981–2005) 21^{st} century, under RCP2.6, RCP4.5 and RCP8.5 warming scenarios are displayed respectively in Fig 8 and 9. For each panel, rows 1-3 represent climate change signals when REMO is forced by EC-Earth (REMO-EC) while rows 4-6 are those of MPI-ESM (REMO-MPI). In all experiments, a significant decrease of wet days frequency along equatorial regions ($\sim$40%) is found during DJF under the three scenarios. During MAM, decrease in REMO-MPI is more perceptible than in REMO-EC with a slight intensification at late 21^{st} century. In general, projections of both runs are similar for the two projected periods: an increase in frequency of wet days over coastal countries ($\sim$80%) is noted, and decrease is recorded according to all scenarios. In a previous study, Fotso-Nguemo et al (2016) had found a projected decrease in mean precipitation over CA under RCP2.6 and RCP4.5. Moreover, the future atmosphere over CA is projected to be drier (Laprise et al, 2013; Fotso-Nguemo et al, 2016; Pokam et al, 2018). These contexts are in good agreement with our findings. The decrease found in the mean rainfall can be associated with the decrease of number of wet days as suggested by Cayan et al (2008). Some differences are noticeable amongst various REMO's RCP forcings with regard to the spatial extent of the frequency of wet days over the continent: during MAM in mid-century, REMO-EC shows an increase in frequency of wet days over Reg 1 (Sahelian region, $\sim$10%) which on the contrary decreases in REMO-MPI. Likewise, in the eastern sector, the frequency of wet days tends to decrease toward the higher global warming scenarios. Sylla et al (2010) using RegCM3, found that anthropogenic greenhouse gases induced global warming, leading to drier conditions over most of West Africa, and especially over the Sahel.

3.2.2 Change in threshold of extreme rainfall

Figure 10 shows projections (**a** 2041–2065 minus 1981–2005 and **b** 2071–2095 minus 1981–2005) in the threshold of extreme events, for both REMO setups under the three RCPs warming scenarios. They all project a decrease of the threshold of extreme events over sahelian regions ($\sim$40%) and east of CA ($\sim$60%). Changes are more intense under REMO-MPI's RCPs. An increase of threshold is found over coastal regions with moderate intensity toward the inland. A dipole change signal appears between the northern DRC and sahelian regions. There is an opposite response on the climate change signal between coastal countries and interior of the continent (northern and eastern CA). Over most part of the DRC, an increase of extreme events threshold can be noted at the late century, but more pronounced in REMO-EC's RCPs while those of REMO-MPI show a decrease. A reverse situation prevails over the East of the study area. These results are similar to those found in previous studies e.g. (Fotso-Nguemo et al, 2017). This is potentially linked to the moisture feedback which strongly influences depending on the convective scheme used (Saeed et al, 2013; Mariotti et al, 2014).

3.2.3 Change in cumulative frequency of daily rainfall

The climate change signal (**a** 2041–2065 minus 1981–2005 and **b** 2071–2095 minus 1981–2005) in the cumulative frequency of daily rainfall is shown in Fig 11. The projected distribution of rainfall intensity look the same for different REMO simulations. Note that a slight variation of rate of decrease rainfall with an increasing intensity corresponds to a considerable change in rainfall intensity. Although all RCPs have different climatic conditions, they agree on a lowering of the rate of decrease rainfall with an increasing intensity. At a scale of the whole CA and for the two projected periods, all REMO-MPI's scenarios plan for a decrease of rate more pronounced under RCP8.5 whereas REMO-EC's scenarios are close to the baseline period. Higher rates are found in Reg 1 and 3, which indicate the persistence of low intensity rains. All REMO's RCPs project similar rate in Reg 2, 3 and 4, but slight disparities occur at the late century under REMO-MPI driven by RCP8.5 with lowest rate in Reg 4. Most disagreements are found in Reg 5 for intensities within the range 10-50 mm/day, more pronounced at the late 21^{st} century and with lowest rate in REMO-MPI forced by RCP8.5. For $R90$, all RCPs of both runs indicate a slight increase over the whole CA and in most sub-regions, more robust under REMO-MPI's scenarios.

4 Summary and conclusion

The ability of REMO, driven by MPI-ESM and EC-Earth, to simulated daily characteristics of precipitation over CA was assessed in this study. A comparative analysis among REMO's experiments and three observations have been done. Mean seasonal rainfall, intensity and frequency of wet days, threshold of extreme rainfall and cumulative frequency of daily rainfall were analysed. Climate change responses to the increase GHGs concentration have been investigated under three warming scenarios for the mid (2041–2065) and late (2071–2095) 21^{st} century.

In general, the evaluation shows that REMO can reasonably simulate the geographic features of Central African daily precipitation. Seasonal biases obtained differ in sign, magnitude and patterns between different model forcing experiments. REMO shows wet biases over Ocean and coastal regions. In the continental part of

CA, dry biases seem to be due to LBC and from REMO's internal processes. However over oceanic and coastal regions, the regional model physic is found to dominate over the LBCs. REMO better reproduces the frequency of wet days than their intensity. Moreover, the pattern of intensity of mean precipitation in CA is influenced by the number and intensity of daily rainfall events. It is also found that both REMO simulations succeed to depict the threshold of extreme events with spatial pattern close to all observations. But significant discordances have been recorded on the oceanic regions where simulations strongly overrate thresholds. The observed results in the frequency distribution of daily rainfall show that REMO well splits rainfall amount less than 10 mm/day, but has a relatively low performance for moderate intensities of the order of 20–40 mm/day, and which gradually improves towards the heavy intensities.

The projected frequency of wet days over CA for the two projection periods exhibits a general decrease for all REMO settings and all scenarios, wider under REMO-MPI's RCPs in MAM. These results are consistent with future dry conditions previously projected over CA (Laprise et al, 2013; Fotso-Nguemo et al, 2016, 2017; Pokam et al, 2018). However, CA is projected to moisten in SON. REMO's run settings have shown an opposite climate change signal over sahelian regions in MAM under all RCPs. REMO-EC projects an increase frequency of wet days $\sim$10% while REMO-MPI decrease. Extreme events threshold over sahelian regions are projected to decrease as well as in the eastern part of CA, more significant under REMO-MPI scenarios. Projections of extreme events threshold display a zonal gradient with high values along coastal regions and low values located over DRC. Likewise, a dipole change signal occurs among northern DRC and sahelian regions. All REMO's scenarios agree on a lowering of the rate of decrease rainfall with an increasing intensity more pronounced under RCP8.5, corresponding to a slight increase of $R90$ amount, more robust under REMO-MPI's warming scenarios.

Further researches are required to further understand the uncertainties depicted by the model. It is necessary to investigate the origin of poor performance of REMO' forcings to model the transition Ocean-Continent. Moreover, understanding impacts of future climate changes over CA is important for environmental, hydrological, agricultural and socio-economic applications. The investigation shown here provides evidence that the current localised decrease or increase of precipitation over the studied domain will continue during the 21^{st} century, hence the need to adapt future policy and development plans in the region to address these local and regional scale responses.

Acknowledgments

The REMO datasets were obtained from the Climate Service Center Germany (GERICS) in Hamburg through the project "Climate Change Scenarios for the Congo Basin". The authors would like to thank data providers. This work is part of the International Joint Laboratory's research "Dynamics of Land Ecosystems in Central Africa: A Context of Global Changes" (IJL DYCOCA/LMI DYCOFAC). Our gratitude is expressed to the anonymous reviewer for their constructive and useful suggestions.

References

Abiodun BJ, Abba Omar S, Lennard C, Jack C (2015) Using regional climate models to simulate extreme rainfall events in the western cape, south africa. International Journal of Climatology 36(2):689–705, DOI 10.1002/joc.4376, URL http://dx.doi.org/10.1002/joc.4376

Aloysius N, Saiers J (2017) Simulated hydrologic response to projected changes in precipitation and temperature in the congo river basin. Hydrology and Earth System Sciences 21(8):4115–4130, DOI 10.5194/hess-21-4115-2017, URL https://www.hydrol-earth-syst-sci.net/21/4115/2017/

Aloysius NR, Justin S, E SJ, Haibin L, F WE (2015) Evaluation of historical and future simulations of precipitation and temperature in central africa from cmip5 climate models. Journal of Geophysical Research: Atmospheres 121(1):130–152, DOI 10.1002/2015JD023656, URL https://agupubs.onlinelibrary.wiley.com/doi/abs/10.1002/2015JD023656, https://agupubs.onlinelibrary.wiley.com/doi/pdf/10.1002/2015JD023656

Bechtold P, Kohler M, Jung T, Doblas-Reyes F, Leutbecher M, Rodwell MJ, Vitart F, Balsamo G (2008) Advances in simulating atmospheric variability with the ecmwf model: From synoptic to decadal time-scales. Quarterly Journal of the Royal Meteorological Society 134(634):1337–1352, URL https://doi.org/10.1002/qj.289

Birkett C (2000) Synergistic remote sensing of lake chad: Variability of basin inundation. Remote Sensing of Environment 72(2):218–236, URL https://doi.org/10.1175/1520-0493(1989)117<1779:ACMFSF>2.0.CO;2

Cayan DR, Maurer EP, Dettinger MD, Tyree M, Hayhoe K (2008) Climate change scenarios for the california region. Climatic Change 87(1):21–42, DOI 10.1007/s10584-007-9377-6, URL https://doi.org/10.1007/s10584-007-9377-6

Coppola E, Giorgi F, Raffaele F, Fuentes-Franco R, Giuliani G, LLopart-Pereira M, Mamgain A, Mariotti L, Diro GT, Torma C (2014) Present and future climatologies in the phase i crema experiment. Climatic Change 125(1):23–38, DOI 10.1007/s10584-014-1137-9, URL https://doi.org/10.1007/s10584-014-1137-9

Creese A, Washington R (2016) Using qflux to constrain modeled congo basin rainfall in the cmip5 ensemble. Journal of Geophysical Research: Atmospheres 121(22), URL https://doi.org/10.1002/2016JD025596

Creese A, Washington R (2018) A process-based assessment of cmip5 rainfall in the congo basin: the september-november rainy season. Journal of Climate (2018), URL https://doi.org/10.1175/JCLI-D-17-0818.1

Diallo I, Sylla M, Giorgi F, Gaye A, Camara M (2012) Multimodel gcm-rcm ensemble-based projections of temperature and precipitation over west africa for the early 21st century. International Journal of Geophysics 2012, DOI :10.1155/2012/972896, URL http://downloads.hindawi.com/journals/ijgp/2012/972896.pdf

Diallo I, Giorgi F, Deme A, Tall M, Mariotti L, Gaye AT (2016) Projected changes of summer monsoon extremes and hydroclimatic regimes over west africa for the twenty-first century. Climate Dynamics 47(12):3931–3954, DOI 10.1007/s00382-016-3052-4, URL https://doi.org/10.1007/s00382-016-3052-4

Dosio A, Panitz HJ, Schubert-Frisius M, Lüthi D (2015) Dynamical downscaling of cmip5 global circulation models over cordex-africa with cosmo-clm: evaluation over the present climate and analysis of the added value. Climate Dynamics 44(9):2637–2661, DOI 10.1007/s00382-014-2262-x, URL https://doi.org/10.1007/s00382-014-2262-x

Endris HS, Lennard C, Hewitson B, Dosio A, Nikulin G, Panitz HJ (2016) Teleconnection responses in multi-gcm driven cordex rcms over eastern africa. Climate Dynamics 46(9):2821–2846, DOI 10.1007/s00382-015-2734-7, URL https://doi.org/10.1007/s00382-015-2734-7

Fotso-Nguemo TC, Vondou DA, Tchawoua C, Haensler A (2016) Assessment of simulated rainfall and temperature from the regional climate model remo and future changes over central africa. Climate Dynamics 48(11):3685–3705, DOI 10.1007/s00382-016-3294-1, URL https://doi.org/10.1007/s00382-016-3294-1

Fotso-Nguemo TC, Vondou DA, Pokam WM, Djomou ZY, Diallo I, Haensler A, Tchotchou LAD, Kamsu-Tamo PH, Gaye AT, Tchawoua C (2017) On the added value of the regional climate model remo in the assessment of climate change signal over central africa. Climate Dynamics 49(11):3813–3838, DOI 10.1007/s00382-017-3547-7, URL https://doi.org/10.1007/s00382-017-3547-7

Fotso-Nguemo TC, Chamani R, Yepdo ZD, Sonkoué D, Matsaguim CN, Vondou DA, Tanessong RS (2018) Projected trends of extreme rainfall events from cmip5 models over central africa. Atmospheric Science Letters 19(2), DOI 10.1002/asl.803, URL https://doi.org/10.1002/asl.803

Funk CC, Peterson PJ, Landsfeld MF, Pedreros DH, Verdin JP, Rowland JD, Romero BE, Husak GJ, Michaelsen JC, Verdin AP, et al (2014) A quasi-global precipitation time series for drought monitoring. US Geological Survey Data Series 832(4)

Gao H, Bohn TJ, Podest E, McDonald KC, Lettenmaier DP (2011) On the causes of the shrinking of lake chad. Environmental Research Letters 6(3):034,021, URL http://stacks.iop.org/1748-9326/6/i=3/a=034021

Garcin Y, Deschamps P, Ménot G, de Saulieu G, Schefuß E, Sebag D, Dupont LM, Oslisly R, Brademann B, Mbusnum KG, Onana JM, Ako AA, Epp LS, Tjallingii R, Strecker MR, Brauer A, Sachse D (2018) Early anthropogenic impact on western central african rainforests 2,600 y ago. Proceedings of the National Academy of Sciences DOI 10.1073/pnas.1715336115, URL http://www.pnas.org/content/early/2018/02/16/1715336115, http://www.pnas.org/content/early/2018/02/16/1715336115.full.pdf

Giorgi F, Jones C, Asrar GR, et al (2009) Addressing climate information needs at the regional level: the cordex framework. World Meteorological Organization (WMO) Bulletin 58(3):175, URL http://wcrp.ipsl.jussieu.fr/cordex/documents/CORDEXgiorgiWMO.pdf

Giorgi F, Coppola E, Raffaele F, Diro GT, Fuentes-Franco R, Giuliani G, Mamgain A, Llopart MP, Mariotti L, Torma C (2014) Changes in extremes and hydroclimatic regimes in the crema ensemble projections. Climatic Change 125(1):39–51, DOI 10.1007/s10584-014-1117-0, URL https://doi.org/10.1007/s10584-014-1117-0

Haensler A, Saeed F, Jacob D (2013) Assessing the robustness of projected precipitation changes over central africa on the basis of a multitude of global and regional climate projections. Climatic Change 121(2):349–363, DOI 10.1007/s10584-013-0863-8, URL https://doi.org/10.1007/s10584-013-0863-8

Hagemann S (2002) An improved land surface parameter dataset for global and regional climate models. MPI Report No 336; Max Planck Institute for Meteorology: Hamburg, Germany URL http://hdl.handle.net/11858/00-001M-0000-002B-539B-6

Hernández-Díaz L, Laprise R, Sushama L, Martynov A, Winger K, Dugas B (2013) Climate simulation over cordex africa domain using the fifth-generation canadian regional climate model (crcm5). Climate Dynamics 40(5):1415–1433, DOI 10.1007/s00382-012-1387-z, URL https://doi.org/10.1007/s00382-012-1387-z

Hua W, Zhou L, Chen H, Nicholson SE, Raghavendra A, Jiang Y (2018) Possible causes of the central equatorial african long-term drought. Environmental Research Letters 11(12):124,002, URL http://stacks.iop.org/1748-9326/11/i=12/a=124002

Huffman GJ, Bolvin DT (2013) Trmm and other data precipitation data set documentation. NASA, Greenbelt, USA 28

Huffman GJ, Adler R, Arkin A, Chang A, Ferraro R, Gruber A, Janowiak J, Mcnab A, Rudolf B, Schneider U (1997) The global precipitation climatology project (gpcp) combined precipitation data set. Bull Am Meteor Soc 78:5?20, URL https://doi.org/10.1175/1520-0477(1997)078\textless0005:TGPCPG\textgreater2.0.CO;2

Ilyina T, Six KD, Segschneider J, Maier-Reimer E, Li H, Núñez-Riboni I (2013) Global ocean biogeochemistry model hamocc: Model architecture and performance as component of the mpi-earth system model in different cmip5 experimental realizations. Journal of Advances in Modeling Earth Systems 5(2):287–315, URL https://doi.org/10.1029/2012MS000178

IPCC (2007) Summary for policymakers. in: Solomon s, qin d, manning m, chen z, marquis m, averyt kb, tignor m, miller hl (eds) climate change 2007: the physical science basis contribution of working group i to the fourth assessment report of the intergovernmental panel on climate change. cambridge university press, cambridge, united kingdom and new york, ny, usa ob c (2001) the representation of cloud cover in atmospheric. Jelektronnyj resurs URL http://www.ipcc.ch

Jackson B, Nicholson SE, Klotter D (2009) Mesoscale convective systems over western equatorial africa and their relationship to large-scale circulation. Monthly Weather Review 137(4):1272–1294, URL https://doi.org/10.1175/2008MWR2525.1

Jacob D, Podzun R (1997) Sensitivity studies with the regional climate model remo. Meteorology and Atmospheric Physics 63(1):119–129, DOI 10.1007/BF01025368, URL https://doi.org/10.1007/BF01025368

James R, Washington R, Rowell DP (2013) Implications of global warming for the climate of african rainforests. Phil Trans R Soc B 368(1625):20120,298, DOI doi:10.1098/rstb.2012.0298, URL http://dx.doi.org/10.1098/rstb.2012.0298

Klutse NAB, Sylla MB, Diallo I, Sarr A, Dosio A, Diedhiou A, Kamga A, Lamptey B, Ali A, Gbobaniyi EO, Owusu K, Lennard C, Hewitson B, Nikulin

G, Panitz HJ, Büchner M (2016) Daily characteristics of west african summer monsoon precipitation in cordex simulations. Theoretical and Applied Climatology 123(1):369–386, DOI 10.1007/s00704-014-1352-3, URL https://doi.org/10.1007/s00704-014-1352-3

Laprise R, Hernández-Díaz L, Tete K, Sushama L, Šeparović L, Martynov A, Winger K, Valin M (2013) Climate projections over cordex africa domain using the fifth-generation canadian regional climate model (crcm5). Climate Dynamics 41(11):3219–3246, DOI 10.1007/s00382-012-1651-2, URL https://doi.org/10.1007/s00382-012-1651-2

Lohmann U, Roeckner E (1996) Design and performance of a new cloud microphysics scheme developed for the echam general circulation model. Climate Dynamics 12(8):557–572, DOI 10.1007/BF00207939, URL https://doi.org/10.1007/BF00207939

Louis JF (1979) A parametric model of vertical eddy fluxes in the atmosphere. Boundary-Layer Meteorology 17(2):187–202, DOI 10.1007/BF00117978, URL https://doi.org/10.1007/BF00117978

Majewski D (1991) The europa-model of the deutscher wetterdienst. ECMWF Seminar Proceedings, Numerical methods in atmospheric models 2:147–191, URL https://ci.nii.ac.jp/naid/10006913190/en/

Malhi Y (2018) Ancient deforestation in the green heart of africa. Proceedings of the National Academy of Sciences DOI 10.1073/pnas.1802172115, URL http://www.pnas.org/content/early/2018/03/15/1802172115, http://www.pnas.org/content/early/2018/03/15/1802172115.full.pdf

Mariotti L, Diallo I, Coppola E, Giorgi F (2014) Seasonal and intraseasonal changes of african monsoon climates in 21st century cordex projections. Climatic Change 125(1):53–65, DOI 10.1007/s10584-014-1097-0, URL https://doi.org/10.1007/s10584-014-1097-0

Mikolajewicz U, Notz D, von Storch J (2010) Characteristics of the ocean simulations in mpiom, the ocean component of the mp earth system model. J Adv Model Earth Syst Kageyama M, Paul A, Roche DM, Van Meerbeeck CJ

Morcrette JJ (1991) Radiation of cloud radiative properties in the European Centre for Medium Range Weather Forecasts forecasting system. Journal of Geophysical Research 96(5):9121–9132

Moss RH, Edmonds JA, Hibbard KA, Manning MR, Rose SK, Van Vuuren DP, Carter TR, Emori S, Kainuma M, Kram T, et al (2010) The next generation of scenarios for climate change research and assessment. Nature 463(7282):747–756

Nicholson SE, Grist JP (2003) The seasonal evolution of the atmospheric circulation over west africa and equatorial africa. Journal of Climate 16(7):1013–1030, URL https://doi.org/10.1175/1520-0442(2003)016$\textless$1013:TSEOTA$\textgreater$2.0.CO;2

Nikulin G, Jones C, Giorgi F, Asrar G, Büchner M, Cerezo-Mota R, Christensen OB, Déqué M, Fernandez J, Hänsler A, et al (2012) Precipitation climatology in an ensemble of cordex-africa regional climate simulations. Journal of Climate 25(18):6057–6078, DOI 10.1175/JCLI-D-11-00375.1, URL https://doi.org/10.1175/JCLI-D-11-00375.1

Panitz HJ, Dosio A, Büchner M, Lüthi D, Keuler K (2014) Cosmo-clm (cclm) climate simulations over cordex-africa domain: analysis of the era-interim driven simulations at 0.44 degree and 0.22 degree resolution. Climate Dynamics 42(11):3015–3038, DOI 10.1007/s00382-013-1834-5, URL https://doi.org/10.1007/s00382-013-1834-5

Pokam WM, Longandjo GN, Moufouma-Okia W, Bell JP, James R, Vondou DAD, Haensler A, Nguemo TCF, Guenang GM, Tchotchou ALD, Kamsu-Tamo PH, Takong RR, Nikulin G, Lennard C, Dosio A (2018) Consequences of 1.5°c and 2°c global warming levels for temperature and precipitation changes over central africa. Environmental Research Letters URL http://iopscience.iop.org/10.1088/1748-9326/aab048

Reick C, Raddatz T, Brovkin V, Gayler V (2013) Representation of natural and anthropogenic land cover change in mpi-esm. Journal of Advances in Modeling Earth Systems 5(3):459–482, URL https://doi.org/10.1002/jame.20022

Saeed F, Haensler A, Weber T, Hagemann S, Jacob D (2013) Representation of extreme precipitation events leading to opposite climate change signals over the congo basin. Atmosphere 4(3):254–271, DOI 10.3390/atmos4030254, URL http://www.mdpi.com/2073-4433/4/3/254

Sylla M, Giorgi F, Coppola E, Mariotti L (2013) Uncertainties in daily rainfall over africa: assessment of gridded observation products and evaluation of a regional climate model simulation. International Journal of Climatology 33(7):1805–1817, DOI 10.1002/joc.3551

Sylla MB, Gaye AT, Jenkins GS, Pal JS, Giorgi F (2010) Consistency of projected drought over the sahel with changes in the monsoon circulation and extremes in a regional climate model projections. Journal of Geophysical Research: Atmospheres (1984?2012) 115(D16), DOI 10.1029/2009JD012983, URL http:https://doi.org/10.1029/2009JD012983

Sylla MB, Giorgi F, Pal JS, Gibba P, Kebe I, Nikiema M (2015) Projected changes in the annual cycle of high intensity precipitation events over west africa for the late 21st century. Journal of Climate 28(2015), DOI 10.1175/JCLI-D-14-00854.1, URL https://doi.org/10.1175/JCLI-D-14-00854.1

Taylor KE, Stouffer RJ, Meehl GA (2012) An overview of cmip5 and the experiment design. Bulletin of the American Meteorological Society 93(4):485, DOI 10.1175/BAMS-D-11-00094.1, URL https://doi.org/10.1175/BAMS-D-11-00094.1

Teichmann C, Eggert B, Elizalde A, Haensler A, Jacob D, Kumar P, Moseley C, Pfeifer S, Rechid D, Remedio AR, Ries H, Petersen J, Preuschmann S, Raub T, Saeed F, Sieck K, Weber T (2013) How does a regional climate model modify the projected climate change signal of the driving gcm: A study over different cordex regions using remo. Atmosphere 4(2):214–236, DOI 10.3390/atmos4020214, URL http://www.mdpi.com/2073-4433/4/2/214

Tiedtke M (1989) A comprehensive mass flux scheme for cumulus parameterization in large-scale models. Monthly Weather Review 117(8):1779 – 1800, URL https://doi.org/10.1175/1520-0493(1989)117\textless1779:ACMFSF\textgreater2.0.CO;2

Van Noije T, Le Sager P, Segers A, van Velthoven P, Krol M, Hazeleger W, Williams A, Chambers S (2014) Simulation of tropospheric chemistry and aerosols with the climate model ec-earth. Geosci Model Dev Discuss 7:1933–2006

Vondou DA, Haensler A (2017) Evaluation of simulations with the regional climate model remo over central africa and the effect of increased spatial resolution. International Journal of Climatology URL https://doi.org/10.1002/joc.5035

Washington R, James R, Pearce H, Pokam WM, Moufouma-Okia W (2013) Congo basin rainfall climatology: can we believe the climate models? Philosophical Transactions of the Royal Society of London B: Biological Sciences 368(1625), DOI 10.1098/rstb.2012.0296, URL http://rstb.royalsocietypublishing.org/content/368/1625/20120296, http://rstb.royalsocietypublishing.org/content/368/1625/20120296.full.pdf

Weber T, Haensler A, Jacob D (2017) Sensitivity of the atmospheric water cycle to corrections of the sea surface temperature bias over southern africa in a regional climate model. Climate Dynamics DOI 10.1007/s00382-017-4052-8, URL https://doi.org/10.1007/s00382-017-4052-8

List of Tables

Table 1 Specifications of the Regional Model REMO used for simulations at the regional scale.

Model	Advection Scheme	Convection Scheme	Radiation Scheme	Turbulent Vertical Diffusion	Cloud Microphysics Scheme	Land Surface Scheme
REMO	Semi-Lagrangian	Tiedtke (Tiedtke, 1989)	Morcrette (Morcrette, 1991)	Louis (Louis, 1979)	Lohmann and Roeckner Lohmann and Roeckner (1996)	Hagemann (Hagemann, 2002)

Table 2 Summary of statistical parameters of mean precipitation between REMO models and observations for the whole CA.

		REMO-EC				REMO-MPI			
		DJF	**MAM**	**JJA**	**SON**	**DJF**	**MAM**	**JJA**	**SON**
CHIRPS	Bias (mm/day)	-2.30	2.32	3.01	3.50	-4.15	-2.51	1.06	3.92
	RMSD (mm/day)	1.76	1.62	2.54	2.01	2.12	1.68	2.53	2.01
	PCC	0.94	0.89	0.89	0.94	0.93	0.93	0.88	0.92
GPCP	Bias (mm/day)	5.74	12.02	8.89	10.12	3.37	7.15	7.01	10.15
	RMSD (mm/day)	3.74	2.91	4.42	3.31	3.51	2.95	4.26	3.25
	PCC	0.80	0.76	0.84	0.83	0.80	0.79	0.83	0.83
TRMM	Bias (mm/day)	8.53	15.10	11.94	13.98	6.16	10.23	10.06	14.01
	RMSD (mm/day)	3.69	2.73	4.23	3.17	3.41	2.74	4.07	3.06
	PCC	0.54	0.69	0.53	0.66	0.59	0.70	0.53	0.69

Table 3 Summary of statistical parameters of frequency of wet days between REMO models and observations for the whole CA.

		REMO-EC				REMO-MPI			
		DJF	**MAM**	**JJA**	**SON**	**DJF**	**MAM**	**JJA**	**SON**
CHIRPS	Bias (%)	-2.70	1.84	0.24	0.51	-5.13	-3.78	-3.03	0.56
	PCC	0.94	0.87	0.84	0.88	0.94	0.91	0.83	0.87
GPCP	Bias (%)	5.16	12.96	8.70	10.67	2.73	7.34	5.42	10.72
	PCC	0.86	0.76	0.82	0.85	0.88	0.79	0.81	0.85
TRMM	Bias (%)	7.30	15.39	10.78	14.02	4.87	9.76	7.50	14.07
	PCC	0.86	0.70	0.82	0.84	0.87	0.75	0.81	0.85

Table 4 Summary of statistical parameters of mean intensity of daily rainfall event between REMO models and observations for the whole CA.

		REMO-EC				REMO-MPI			
		DJF	**MAM**	**JJA**	**SON**	**DJF**	**MAM**	**JJA**	**SON**
CHIRPS	Bias (%)	30.43	21.00	10.85	26.79	42.48	21.22	10.08	25.66
	PCC	0.67	0.69	0.61	0.82	0.55	0.74	0.55	0.84
GPCP	Bias (%)	15.39	-8.03	-2.37	9.82	26.05	-7.86	-3.05	8.84
	PCC	0.24	0.45	0.19	0.25	0.15	0.48	0.19	0.22
TRMM	Bias (%)	19.29	-0.10	-1.56	20.83	30.31	0.07	-2.24	19.75
	PCC	0.34	0.57	0.35	0.39	0.27	0.59	0.36	0.38

List of Figures

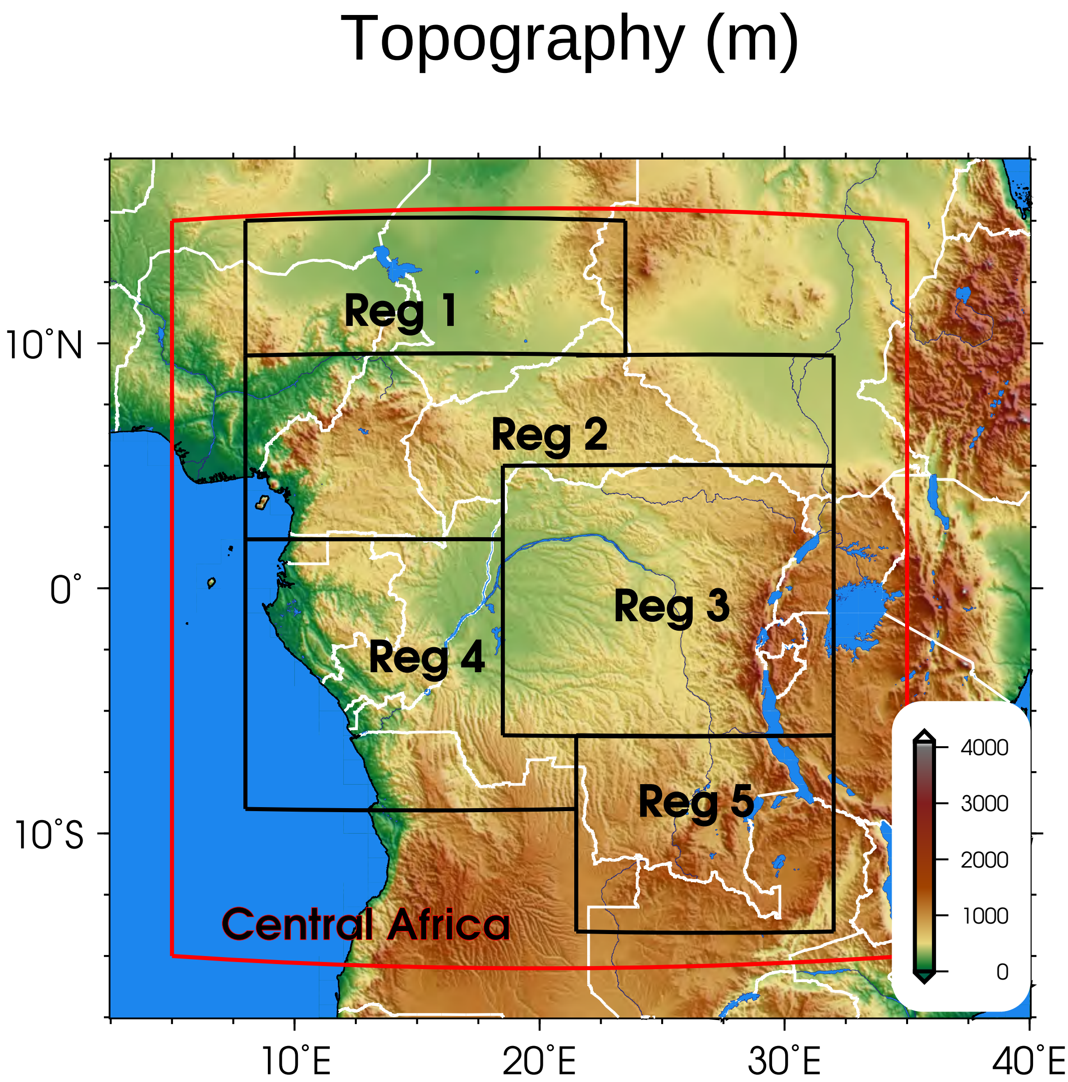

Fig. 1 Study domain covering the Central Africa countries (Red box, 15°S to 15°N – 5° to 35°E). The five black boxes (Regs) are homogeneous areas selected for regional analysis of rainfall. Background: based on 30-arc seconds GTOPO30 Digital Elevation Model.

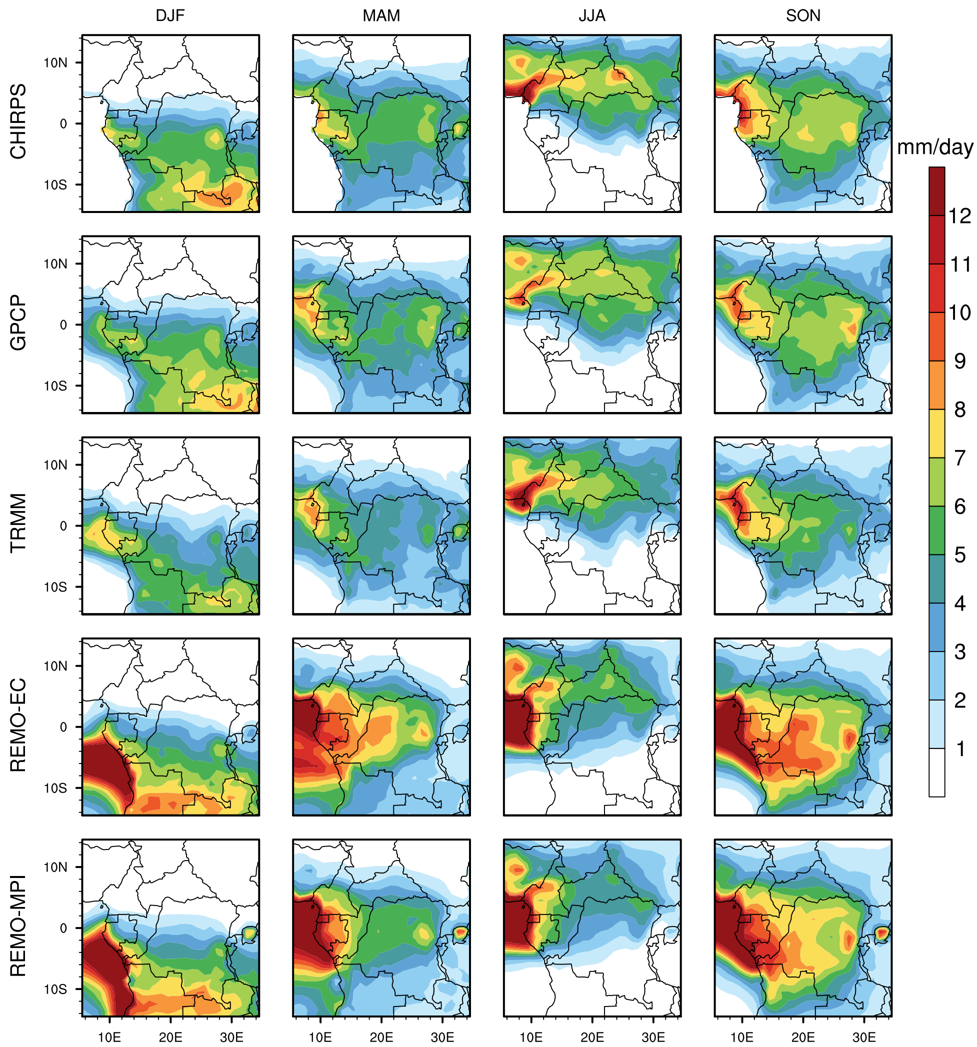

Fig. 2 Seasonal-mean rainfall (in mm/day) under baseline period, from observations CHIRPS (*row 1*), GPCP (*row 2*), TRMM (*row 3*) and from REMO simulations: REMO-EC (*row 4*) and REMO-MPI (*row 5*). Models and CHIRPS observation are averaged for the 1981-2005 period whereas TRMM and GPCP averages cover the 1998 - 2005 periods

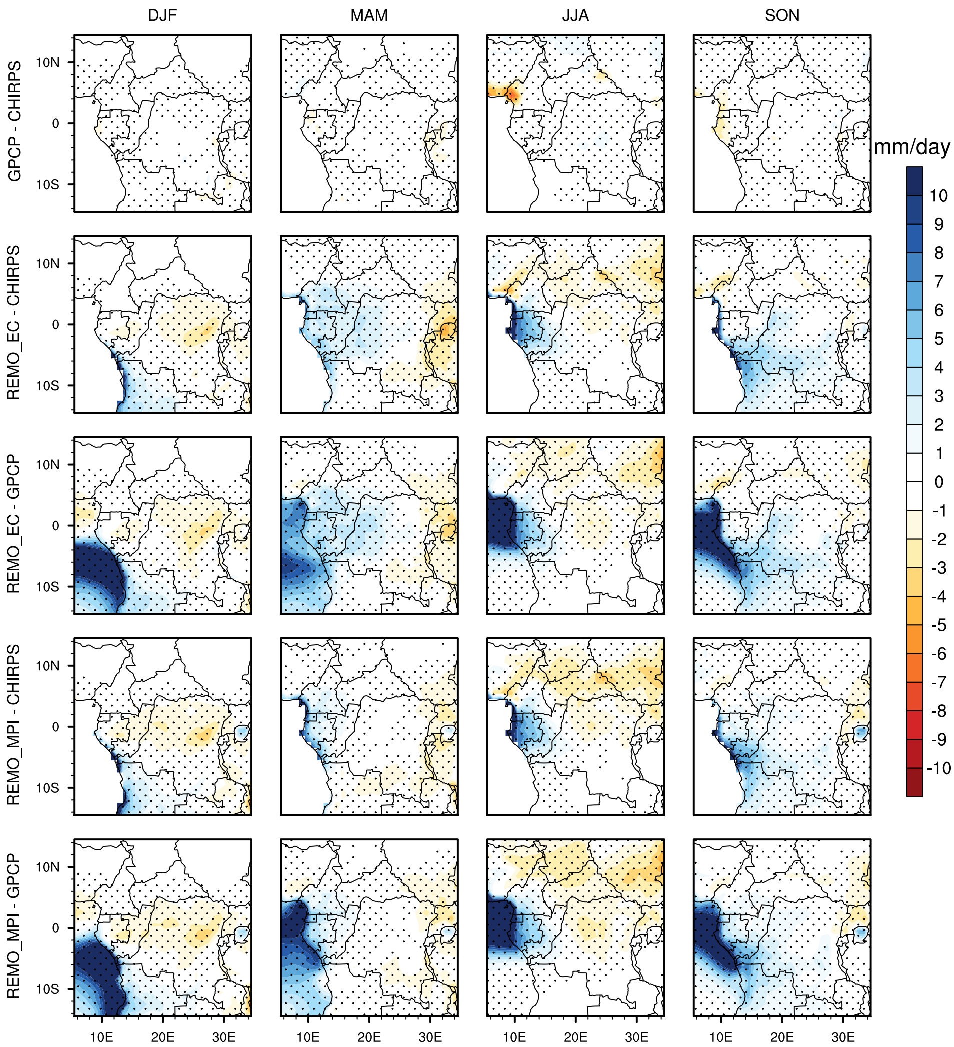

Fig. 3 Mean seasonal rainfall biases (in mm/day). As references, GPCP and CHIRPS are used to account for uncertainties in observed products. Also shown are REMO-EC bias (*rows 2 and 3*) and REMO-MPI bias (*rows 4 and 5*). Stippling indicates 95% significance level using t-test.

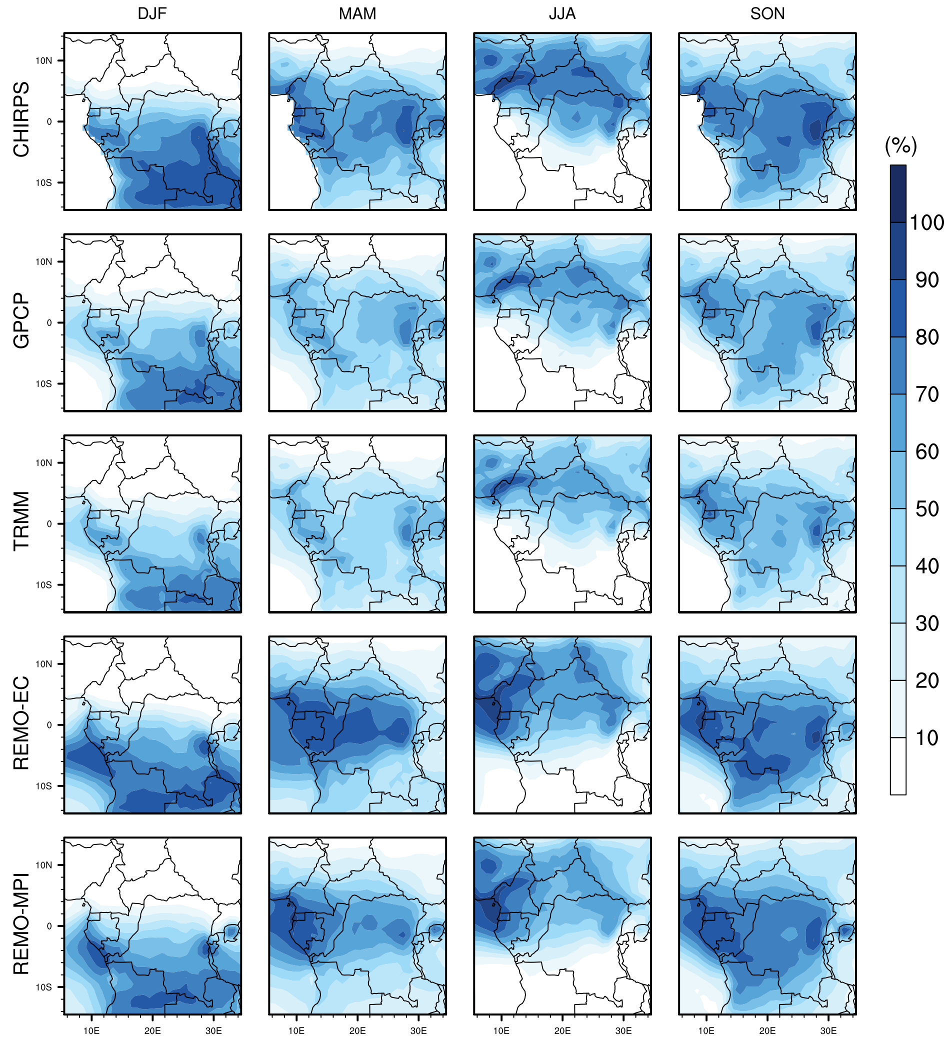

Fig. 4 Seasonal mean frequency of wet days (in % of total annual days) from observations CHIRPS (*row 1*), GPCP (*row 2*), TRMM (*row 3*) and from both REMO outputs: REMO-EC (*row 4*) and REMO-MPI (*row 5*).

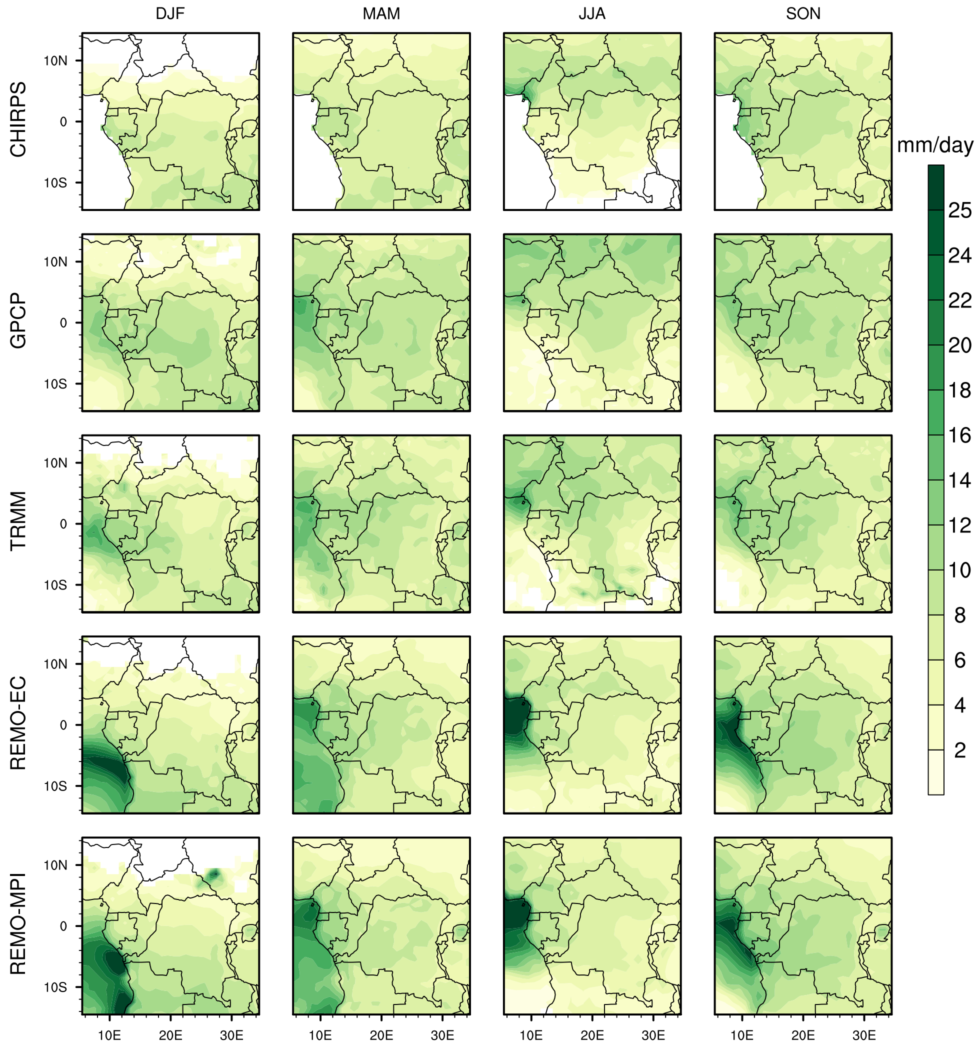

Fig. 5 Mean seasonal intensity of daily rainfall event (in mm/day) from observations CHIRPS (*row 1*), GPCP (*row 2*), TRMM (*row 3*) and from both REMO outputs: REMO-EC (*row 4*) and REMO-MPI (*row 5*).

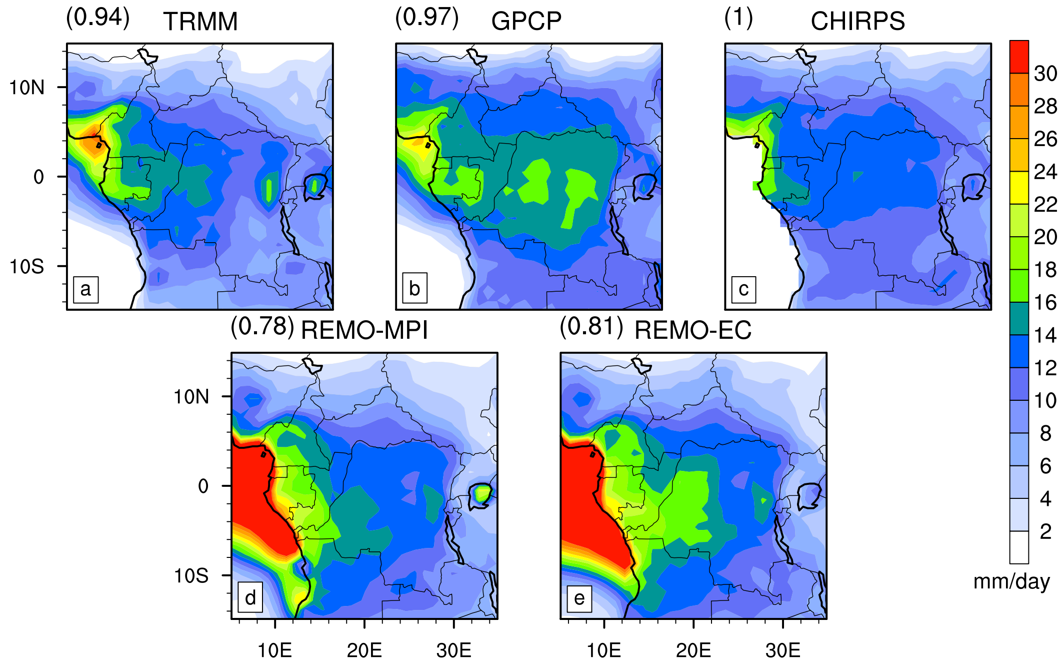

Fig. 6 Threshold of extreme events over CA (i.e. 90^{th} percentile of daily precipitation in mm/day) using observed **a)** TRMM, **b)** GPCP, **c)** CHIRPS and simulated **d)** REMO-MPI and **e)** REMO-EC datasets. The top left values are PCC computed with respect to CHIRPS observation.

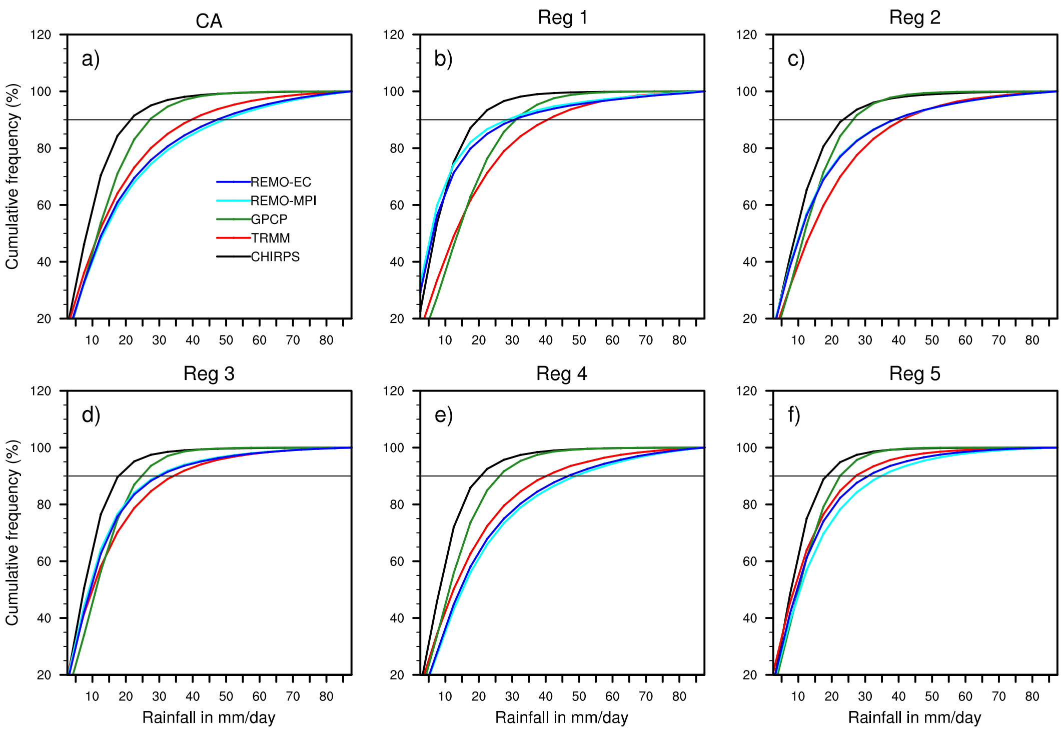

Fig. 7 Frequency distribution and cumulative frequency of rainfall intensity in **a)** CA and in (**b-f**) five homogeneous regions. As observed data, CHIRPS (**black**), TRMM (**red**), GPCP (**forestgreen**). Simulated data are REMO-EC (**blue**) and REMO-MPI (**green**). The horizontal line indicates the 90^{th} percentile of fallen precipitation.

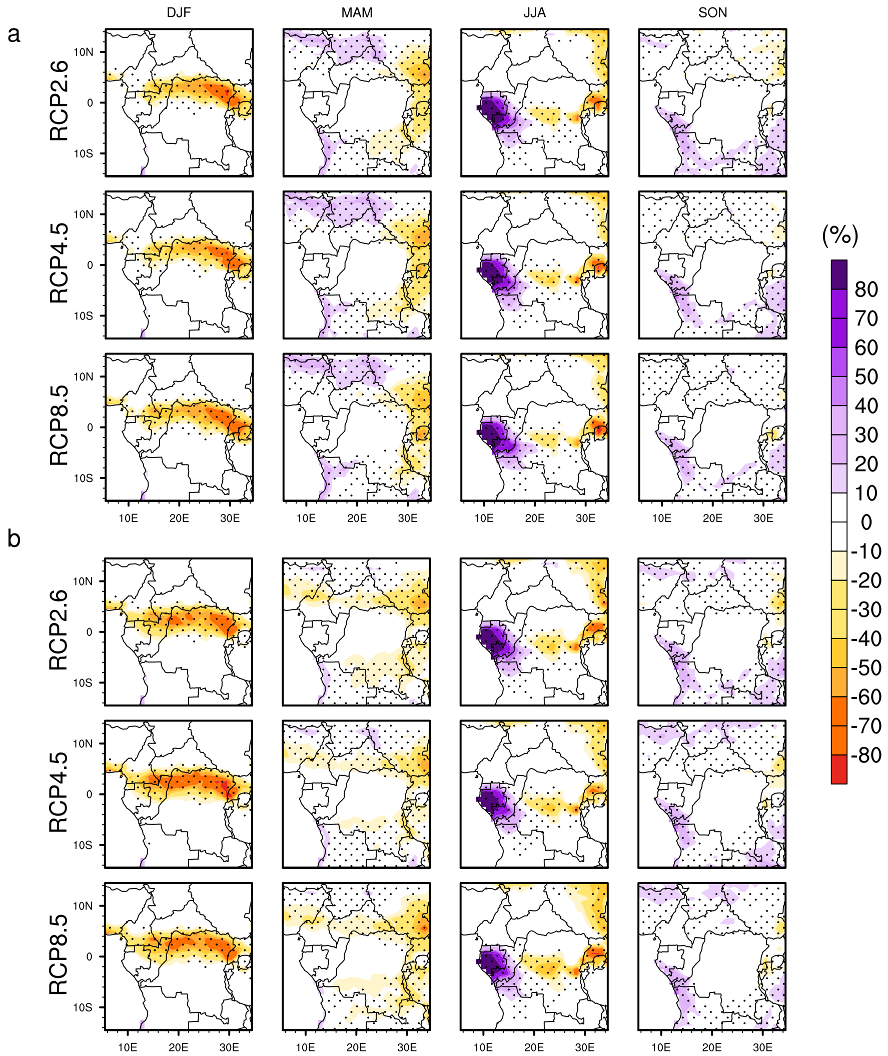

Fig. 8 Projected changes in the mean-seasonal frequency of wet days (in % of total annual days) from **a)** REMO-EC scenarios (RCP2.6 (*row 1*), RCP4.5 (*row 2*), RCP8.5 (*row 3*)) and **b)** REMO-MPI scenarios (RCP2.6 (*row 4*), RCP4.5 (*row 5*), RCP8.5 (*row 6*)) under 2041-2065 period. Stippling indicates 95% significance level using t-test.

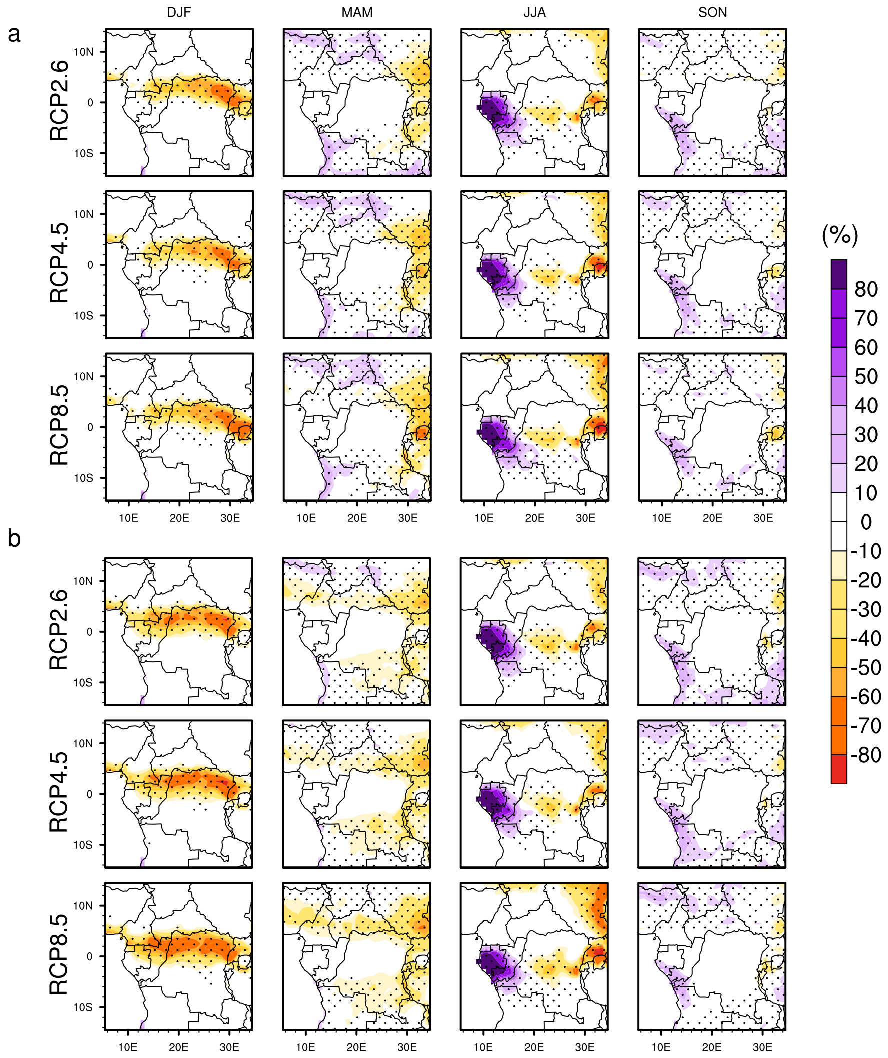

Fig. 9 same as Fig. 8 but under 2071-2095 period.

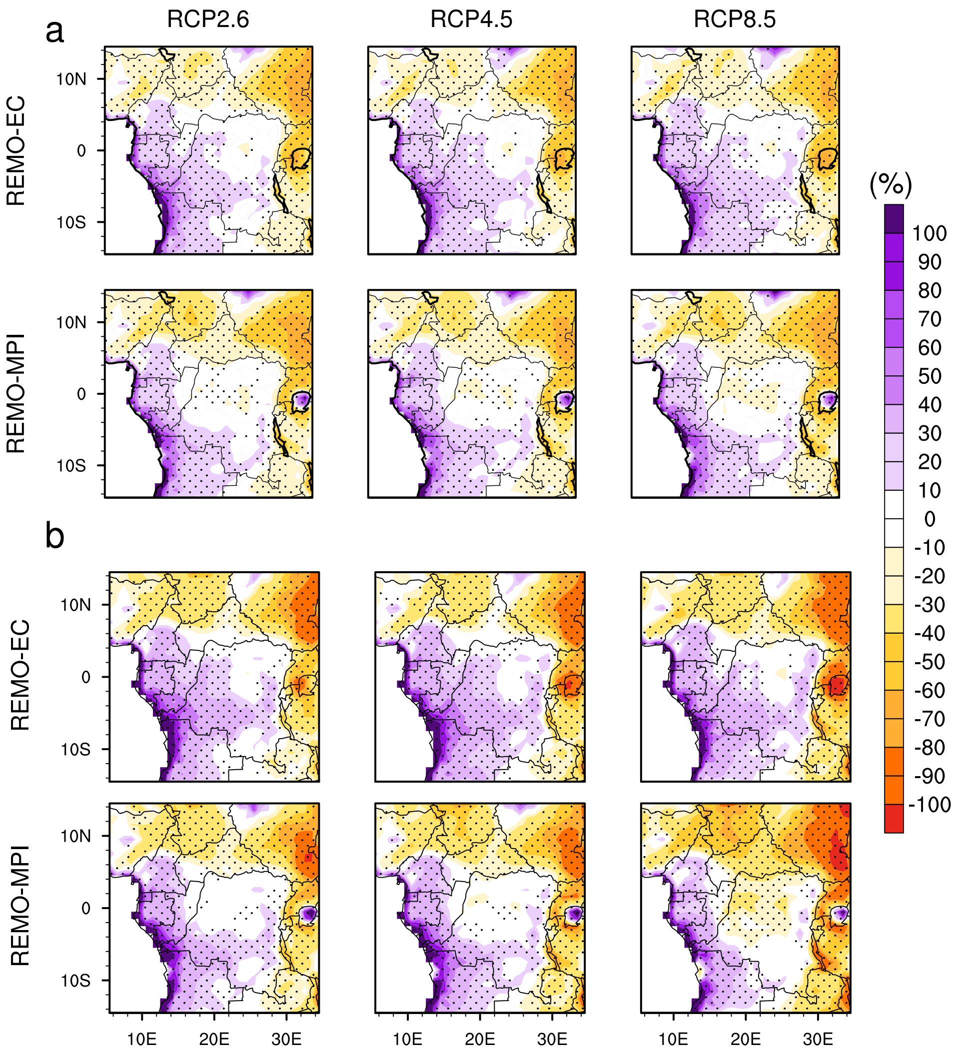

Fig. 10 Projected changes in the threshold of extreme events (in %) from RCP2.6 (*column 1*), RCP4.5 (*column 2*) and RCP8.5 (*column 3*) scenarios of both REMO's outputs (see name left of panel), respectively under **a**) 2041-2065 and **b**) 2071-2095 periods. Stippling indicates 95% significance level using t-test.

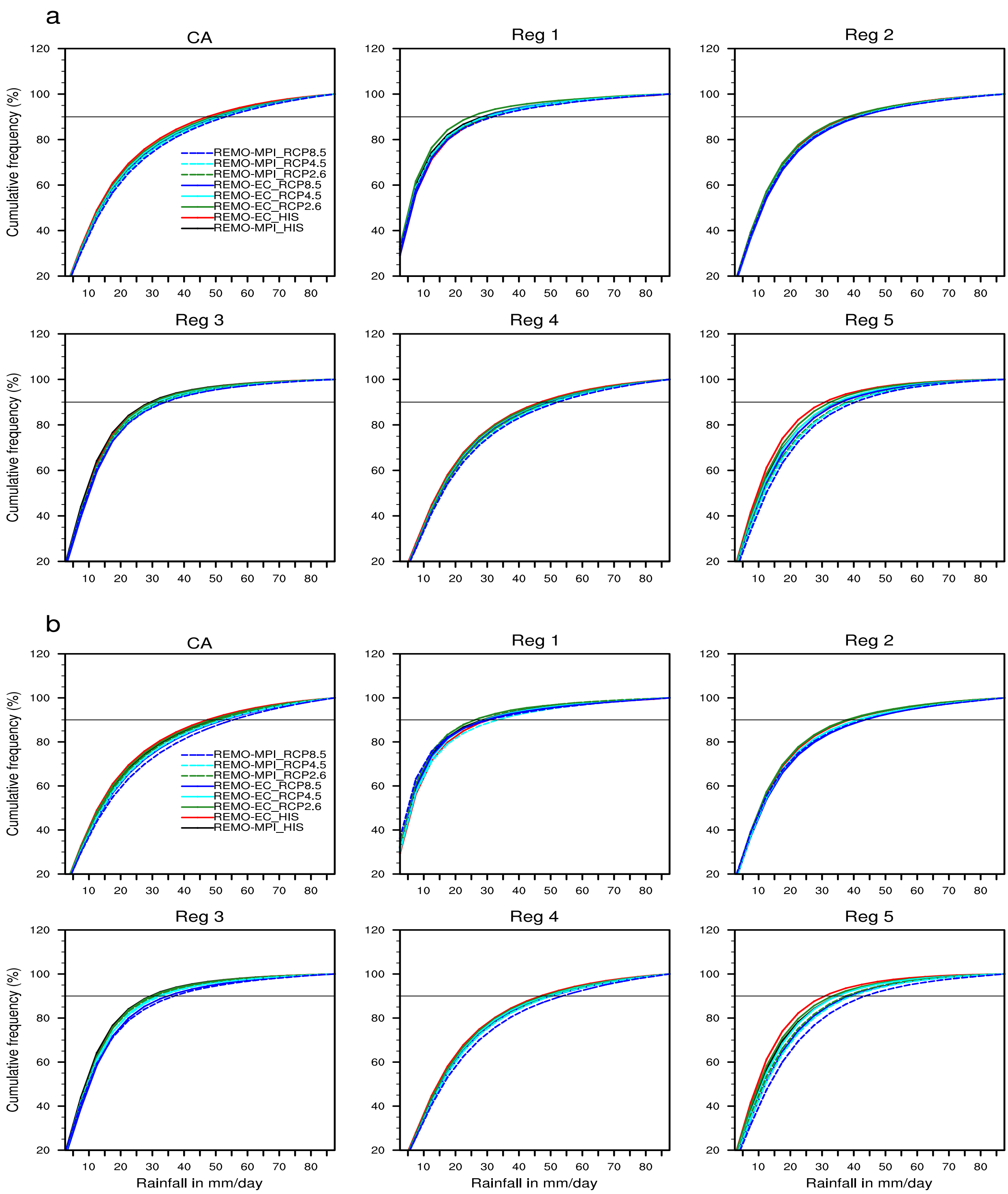

Fig. 11 Projected frequency distribution and cumulative frequency of rainfall intensity over whole CA and homogeneous regions under **a)** 2041-2065 period and **b)** 2071-2095 period, from REMO-EC scenarios (*solid lines*) and REMO-MPI scenarios (*dashed lines*) compared to the historicals (REMO-EC-HIS and REMO-MPI-HIS). The horizontal line indicates the 90^{th} percentile of fallen precipitation.